Relative Role of Stratification and Mixing on the Stability of Linear Detonation Combustors

Michael Ullman, Supraj Prakash, and Venkat Raman

University of Michigan, Ann Arbor, MI, USA

1 Introduction

The performance of detonative combustors is known to be highly sensitive to reactant mixedness and inflow boundary conditions [1]. While detonation theory and many fundamental studies consider premixed reactants, most practical systems implement non-premixed injection for safety considerations. As a result, these systems are plagued by incomplete reactant mixing, and the wave speeds and peak pressures are often considerably lower than the Chapman-Jouguet (CJ) speed and von Neumann pressure [2, 3]. Insufficient mixing can prevent waves from fully consuming the reactants they encounter, causing the energy release behind the waves to be lower in intensity and more spatially diffuse [4, 5]. Unconsumed reactants are then able to mix with hot residual product gases, facilitating deflagration ahead of the primary detonation waves. This parasitic combustion [6] also works to weaken the detonation waves by partially consuming and preheating the reactant mixture. Similar to mixing deficiency, this process leads to weaker heat release behind the waves, which takes place over a broadened reaction zone [5]. Thus, the composition of the reactant mixture, and the way it is provided to the combustion chamber, can be expected to have a leading-order effect on the wave dynamics in a detonation combustor.

These non-idealities were noted in experimental [7] and numerical [8] studies of a non-premixed reflective shuttling detonation combustor (RSDC). This setup used a rectangular combustion chamber, with a closed wall on one side and open boundaries on the top and opposite side. For a variety of equivalence ratios, continuous self-excited wave generation and propagation were observed. These waves tended to move at speeds 54-77% of the CJ speeds, likely due to mixture stratification and parasitic deflagration ahead of the waves. While the impact of the reactant mixture on the wave speed, strength, and structure could be inferred from these studies, the role of mixture in facilitating the continuous generation of new waves was less clear. To address this, the present study considers the same RSDC design subject to different modes of fuel and oxidizer injection. First, the reactant manifolds are entirely removed to investigate the impacts of discrete injection and manifold dynamics. Then, premixed reactants are supplied through the reactant manifolds to isolate the effects of reactant mixedness in the combustion chamber. Finally, an additional non-premixed simulation is conducted to ensure the efficacy of a boundary condition imposed in the premixed case.

2 Flow Configurations

The full RSDC geometry is shown in Fig. 1 with an instantaneous pressure field from the baseline non-premixed simulation overlaid on the combustion chamber [8]. In the open-closed configuration, the top

Correspondence to: mullman@umich.edu

and right sides of the chamber are open boundaries and the left side is a wall. The oxidizer enters the chamber through a segmented slot, which is 0.76 mm wide at the chamber base. The fuel is supplied by 53 staggered pairs of cylindrical injectors, which are 1.27 mm in diameter. Not shown in Fig. 1 is the large exhaust plenum that was added outside of the open chamber boundaries to prevent non-physical boundary interactions. The modified geometry uses the same combustion chamber dimensions as the full geometry, but the reactant manifolds and injectors are omitted. Instead, a continuous slot inlet is placed at the bottom of the chamber, which spans the same length as the oxidizer slot in the full geometry. As in the other setup, the top of the chamber is an open boundary and the left side is a wall. Meanwhile, the right side is an open boundary in the open-closed configuration and a wall in the closed-closed configuration. A large exhaust plenum is placed outside of the open boundaries as well.

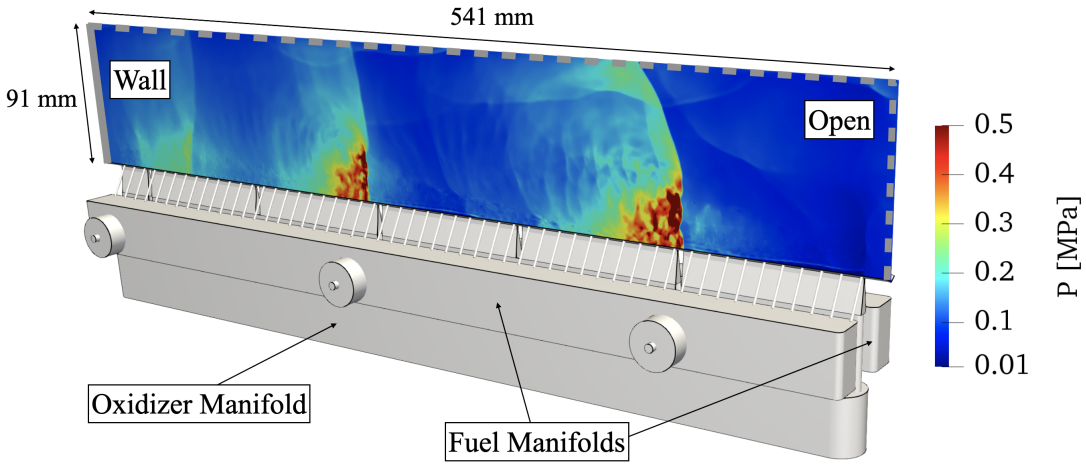

Figure 1: Diametric view of full RSDC geometry, with case 0 pressure field overlaid. Oxidizer enters combustion chamber through segmented slot. Fuel is injected through 106 cylindrical injectors.

For consistency with the previous analyses, the same mesh resolutions are used. In both geometries, 200 μm and 400 μm resolutions are prescribed respectively in the lower and upper halves of the combustion chamber. These resolutions are similar to those implemented in other simulations of detonation combustors [9, 10]. In the full geometry, a 200 μm resolution is also prescribed in the fuel injectors and oxidizer slot. To dissipate outgoing waves, the cells are further coarsened in the exhaust plenums. Together, the chosen mesh resolutions yield 62.5 million cells in the full open-closed setup, 40.5 million cells in the modified open-closed setup, and 38 million cells in the modified closed-closed setup.

The simulation configurations are summarized in Table 1. Case 0 is the baseline case from previous work [8]. Cases I and II use the modified geometry, where the slot inlet supplies premixed reactants at the specified equivalence ratio. Case III uses the same flow rates at the manifold inlets as the baseline case, but the reactants are premixed. To prevent combustion within the manifolds, the reactions are only progressed above the base of the combustion chamber. This enables the investigation of premixed injector dynamics and the effects on the combustion behavior in the chamber alone. To ensure this has no secondary effects on the injector or manifold dynamics, case IV implements the chamber reaction limitation with same flow conditions as case 0.

The initialization is similar for all cases. In cases 0, III, and IV, the manifolds are set to their respective pressures and chemical compositions at 300 K. In all cases, the rest of the domain is prescribed as air at 1 atm and 300 K. The manifold inlets in cases 0, III, and IV are given choked mass flow conditions, while the slot inlet in cases I and II use a total pressure condition. At each inlet boundary face, this condition ensures that the flow is choked unless the neighboring internal cell exceeds the choking pressure. If the neighboring cell pressure is greater than the choking pressure but less than the inlet total pressure, the

boundary face acts as an inlet at the neighboring cell pressure. If the inlet total pressure is exceeded, the boundary face acts as a wall. All of the walls are prescribed no-slip and adiabatic conditions, while the far-field boundaries of the exhaust plenum are subsonic outlets at 1 atm. The flow field is first allowed to develop for 0.5 ms, after which a 3 cm $\times$ 1 cm detonation ramp profile is patched into the bottom of the chamber near the closed end. The simulations are then run for an additional 4.5 ms to allow the steady-state wave behavior to develop.

Table 1: Simulation configurations.

Case	ϕ	Fuel Flow Rate [kg/s]	Oxi. Flow Rate [kg/s]	Manifold Pressure [MPa]	Chamber Ends	Injection Method	Injection Scheme	Reaction Location
0	0.82	0.081	0.394	0.361	O-C	Discrete	Non-PM	All
I	0.80	0.079	0.396	-	O-C	Slot	PM	All
II	0.80	0.079	0.396	-	C-C	Slot	PM	All
III	0.82	0.081	0.394	0.361	O-C	Discrete	PM	Chamber
IV	0.82	0.081	0.394	0.361	O-C	Discrete	Non-PM	Chamber

3 Numerical Methods

The simulation approach solves the full compressible, reacting Navier-Stokes equations with no sub-grid scale turbulence models. The governing mass, momentum, energy, and chemical species conservation equations are closed with an ideal gas equation of state. The solver is the in-house finite volume code UMReactingFlow [11], which has been used to study numerous detonation and reacting flow problems [12, 13]. The code implements CUDA-based GPU acceleration of key fluid and chemistry subroutines. The convective fluxes are computed with the Harten-Lax-van Leer-Contact (HLLC) scheme, while the diffusive fluxes are computed using the Kurganov, Noelle, and Petrova (KNP) method [14]. A second-order Runge-Kutta scheme is used for the temporal discretization. The chemical reactions are computed using Cantera [15] and the formulation of Barwey et al. [16], which enables GPU acceleration of chemical source term evaluations. A skeletal mechanism with 13 species and 38 reactions is used to model the chemical kinetics [17, 18]. This mechanism for methane-oxygen detonations has previously been validated in one- and two-dimensional detonation studies [12].

4 Results and Discussion

The wave behavior in the modified geometry is illustrated by the x-t pressure plots in Fig. 2 and instantaneous pressure field in Fig. 3a. In both chamber configurations, the steady-state behavior is qualitatively similar. After the passage of the initial detonation wave, the systems quickly give way to a steady-state operating mode characterized by numerous cross-propagating acoustic waves. Unlike in the baseline case, these waves fail to coalesce into detonation waves. The chamber pressure remains elevated above the ambient, such that the flow is often choked at the upper open boundary. Due to the asymmetry in reflection strength, the waves in case I develop a clear directional preference from the closed end to the open end. In case II, this preference is less evident; however, there does appear to be an increased prevalence of waves moving from right to left. This may be due to the direction of initial detonation wave, which reflects off of the right wall in a manner that instigates a directional preference which is maintained over the duration of the simulation. If the simulation was continued for a longer time, this directional preference may subside, or periodically transition between right-to-left and left-to-right. The primary region of heat release is at the reactant fill height, where combustion is initiated at the contact surface with residual product gases. Above this height, the reactions are largely complete, and the upper portion of the chamber is nearly uniform in temperature and chemical composition.

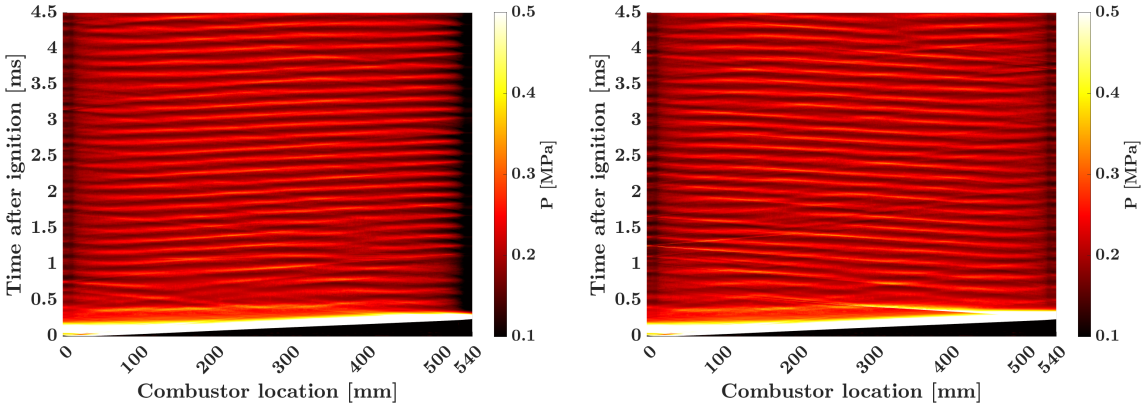

(a) Case I (open-closed, premixed, slot). (b) Case II (closed-closed, premixed, slot).

Figure 2: Mid-plane pressure traces taken 1.11 cm above injection plane in premixed slot cases.

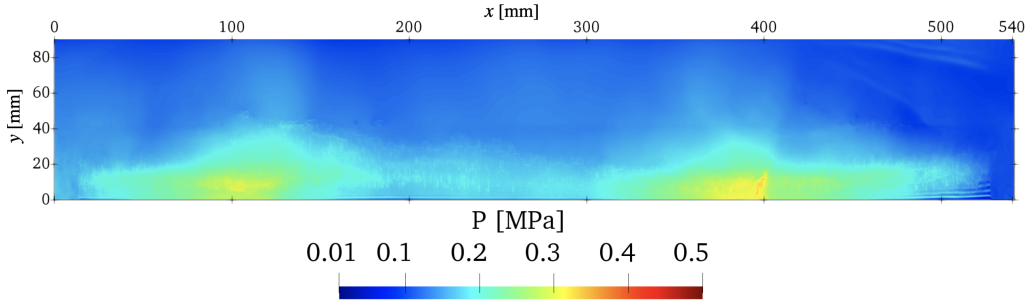

(a) Case I (open-closed, premixed, slot).

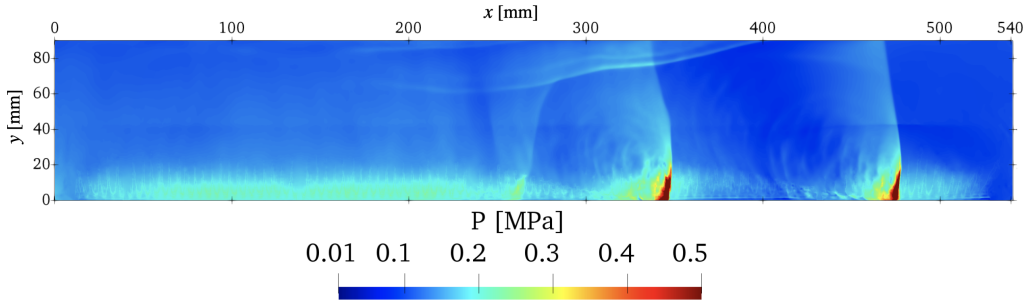

(b) Case III (open-closed, premixed, discrete).

Figure 3: Instantaneous pressure fields in mid-plane of combustion chamber.

The inclusion of discrete injectors in case III gives drastically different wave behavior, as shown in Figs. 3b and 4a. After the initial detonation wave exits the chamber, there is a quiet period while the manifolds recover. Because the oxidizer manifold is suppressed in the wake of the initial wave, its recovery generates waves that enter the chamber and interact with the reflected acoustic waves produced by the initial detonation choking the flow at the open chamber boundaries. Once the reactants are sufficiently replenished, these collisions between waves are able to trigger the formation of detonation waves. These waves traverse the chamber in groups, with each new wave being generated by the coalescence of reflected waves at the ends of the chamber. Roughly 2.5 ms after the emergence of the first waves, the waves exiting the open boundary fail to create additional waves. For the remainder of the simulation, deflagration persists throughout the chamber, and the product gases are directed vertically out of the top

of the chamber. This differs from case IV, where the steady-state wave behavior is qualitatively very similar to the baseline case depicted in Fig. 1. After the manifolds recover and the first waves emerge, there is a period of roughly 2 ms where the left- and right-running waves are of comparable strength. Gradually, this yields to the steady-state behavior, where the directional preference of the waves is evident. Here, acoustic reflections at the open chamber boundaries generate left-running waves, which traverse the chamber, reflect off of the closed end, and strengthen to detonation waves as they move back toward the open end. The similarity between cases 0 and IV suggest that prohibiting chemical reactions in the manifolds has minimal effect on the macroscopic flow features. As a result, the wave behavior observed in case III can be primarily attributed to injector and chamber dynamics.

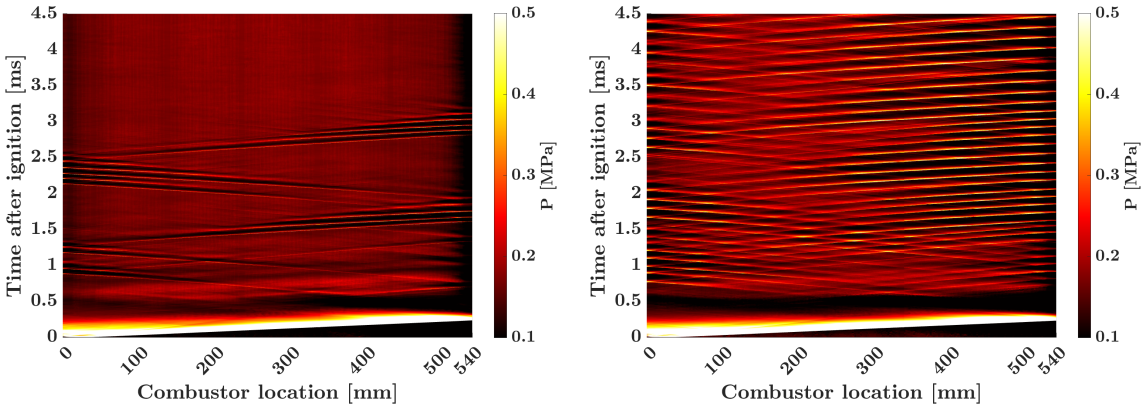

(a) Case III (open-closed, premixed, discrete).

(b) Case IV (open-closed, non-premixed, discrete).

Figure 4: Mid-plane pressure traces taken 1.11 cm above injection plane in full geometry cases.

5 Conclusions

Four configurations of a rectangular reflective shuttling detonation combustor (RSDC) were studied to understand the impact of injection scheme and reactant mixedness on the steady-state wave behavior. The results indicate that both factors play a critical role, and that continuous generation of detonation waves is only present in cases with non-premixed injection from the reactant manifolds. In cases with a premixed slot inlet, the waves fail to coalesce into detonations. Instead, deflagration waves move throughout the chamber, with a directional preference dictated by the asymmetry in chamber boundary condition in the open-closed configuration, and possibly the initialization method in the closed-closed configuration. In the case with premixed reactants supplied by the manifolds, detonations are formed in quick succession following wave reflections and collisions at the ends of the chamber. However, unlike the non-premixed cases, these waves eventually subside, leaving a steady-state of purely deflagrative combustion. Limiting the chemical reactions to above the base of the combustion chamber did not significantly impact the wave dynamics in the non-premixed setup, suggesting that the differences in operating modes in the full geometry are due to injector and chamber dynamics. Further investigation will be required to identify the physical processes leading to the observed differences in macroscopic features. For instance, the premixed fuel and oxidizer are likely more readily consumed via deflagration, leaving less reactants available to support detonation waves. In addition, longer time simulations may explain how or whether the directional preference of the dominant wave system changes in a closed-closed chamber configuration. Together, these analyses may provide insights that can be applied to the design and operation of practical detonation combustor technologies.

References

[1] F. A. Bykovskii, S. A. Zhdan, and E. F. Vedernikov, "Continuous spin detonations," *Journal of propulsion and power*, vol. 22, no. 6, pp. 1204–1216, 2006.

[2] B. A. Rankin *et al.*, "Chemiluminescence imaging of an optically accessible non-premixed rotating detonation engine," *Combust. Flame*, vol. 176, pp. 12–22, 2017.

[3] B. Bigler, J. Bennewitz, S. Danczyk, and W. Hargus, "Rotating detonation rocket engine operability under varied pressure drop injection," *J Spacecr Rockets*, vol. 58, no. 2, pp. 316–325, 2021.

[4] S. Prakash, R. Fiévet, and V. Raman, "The effect of fuel stratification on the detonation wave structure," in *AIAA Scitech 2019 Forum*, 2019, p. 1511.

[5] S. Prakash and V. Raman, "The effects of mixture preburning on detonation wave propagation," *Proc. Combust. Inst.*, vol. 38, no. 3, pp. 3749–3758, 2021.

[6] F. Chacon and M. Gamba, "Study of parasitic combustion in an optically accessible continuous wave rotating detonation engine," in *AIAA Scitech 2019 Forum*, 2019, p. 0473.

[7] A. Lemcherfi *et al.*, "Effect of injection dynamics on detonation wave propagation in a linear detonation combustor," *Proc. Combust. Inst.*, 2022.

[8] M. Ullman, S. Prakash, D. Jackson, V. Raman, C. Slabaugh, and J. Bennewitz, "Self-excited wave propagation in a linear detonation combustor," *In preparation*, 2022.

[9] S. Prakash, R. Fiévet, V. Raman, J. Burr, and K. Yu, "Analysis of the detonation wave structure in a linearized rotating detonation engine," *AIAA Journal*, vol. 58, no. 12, pp. 5063–5077, 2020.

[10] D. Schwer and K. Kailasanath, "Feedback into mixture plenums in rotating detonation engines," in *50th AIAA Aerospace Sciences Meeting*, 2012, p. 617, AIAA Paper 2012-617.

[11] R. Bielawski, S. Barwey, S. Prakash, and V. Raman, "Highly-scalable gpu-accelerated compressible reacting flow solver for modeling high-speed flows," *Submitted to Comput. Fluids*, 2022.

[12] S. Prakash, V. Raman, C. Lietz, W. Hargus, and S. Schumaker, "High fidelity simulations of a methane-oxygen rotating detonation rocket engine," in *AIAA Scitech Forum*, 2020, p. 0689.

[13] T. Sato *et al.*, "Mixing and detonation structure in a rotating detonation engine with an axial air inlet," *Proc. Combust. Inst.*, vol. 38, no. 3, pp. 3769–3776, 2021.

[14] C. Greenshields, H. Weller, L. Gasparini, and J. Reese, "Implementation of semi-discrete, non-staggered central schemes in a colocated, polyhedral, finite volume framework, for high-speed viscous flows," *Int. J. Numer. Methods Fluids*, vol. 63, no. 1, pp. 1–21, 2010.

[15] D. Goodwin, H. Moffat, and R. Speth, "Cantera: an object-oriented software toolkit for chemical kinetics, thermodynamics, and transport processes," https://www.cantera.org, Version 2.3.0., 2017.

[16] S. Barwey and V. Raman, "A neural network-inspired matrix formulation of chemical kinetics for acceleration on GPUs," *Energies*, vol. 14, no. 9, p. 2710, 2021.

[17] R. Xu and H. Wang, "A reduced reaction model of methane combustion," 2018, personal comm.

[18] G. Smith, Y. Tao, and H. Wang, "Foundational fuel chemistry model version 1.0 (ffcm-1)," http://nanoenergy.stanford.edu/ffcm1, 2016.